Electronic Supplementary Information (ESI) for

Fatigue Mechanism of Yttrium-Doped Hafnium Oxide Ferroelectric Thin Films Fabricated by Pulsed Laser Deposition

Fei Huang,[a,b,d] Xing Chen,[f] Xiao Liang,[a,b,d] Jun Qin,[a,b,d] Yan Zhang,[a,b,d] Taixing Huang,[a,b,c,d] Zhuo Wang,[b] Bo Peng,[a,b,d] Peiheng Zhou,[a,b,d] Haipeng Lu,[a,b,d] Li Zhang,[a,b,d] Longjiang Deng,[a,b,d] Ming Liu,[e] Qi Liu,[e,*] He Tian[f,*] and Lei Bi[a,b,d,*]

[a] *National Engineering Research Center of Electromagnetic Radiation Control Materials, University of Electronic Science and Technology of China, Chengdu 610054, China.*

[b] *State Key Laboratory of Electronic Thin Films and Integrated Devices, University of Electronic Science and Technology of China, Chengdu 610054, China.*

[c] *Sichuan Province Key Laboratory of Information Materials and Devices Application, Chengdu University of Information Technology, Chengdu 610225, China*

[d] *Key Laboratory of Multi-spectral Absorbing Materials and Structures of Ministry of Education, University of Electronic Science and Technology of China, Chengdu 610054, China.*

[e] *Key Laboratory of Microelectronics Device & Integrated Technology, Lab of Nanofabrication and Novel Device Integration, IMECAS, Beijing, China.*

[f] *Center of Electron Microscopy and State Key Laboratory of Silicon Materials, School of Materials Science and Engineering, Zhejiang University, Hangzhou 310027, China.*

*E-mail: liuqi@ime.ac.cn, hetian@zju.edu.cn, bilei@uestc.edu.cn.

S1. Evolution of the hysteresis loops with the increase of applied electric field.

Fig. S1 shows the evolution of the sub-loops with the increase of applied electric field of a pristine device.

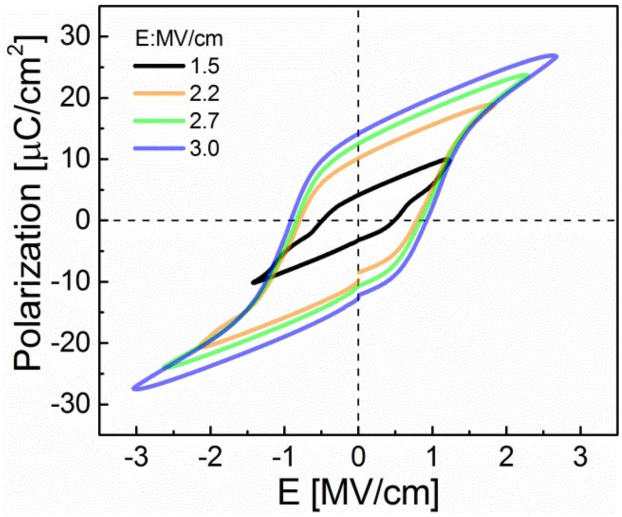

Figure S1. Evolution of the sub-loops with the increase of applied electric field.

S2. Hysteresis loops of different Y doping concentration samples.

We also fabricated films with other doped concentration ranging from 0-12 mol.%. When the doped concentration is 3.8 mol.% films have the best ferroelectricity and the remanent polarization (2Pr) increases to 30 μC/cm². So we used these films as samples to study in this paper. The hysteresis loops are shown in fig. S2.

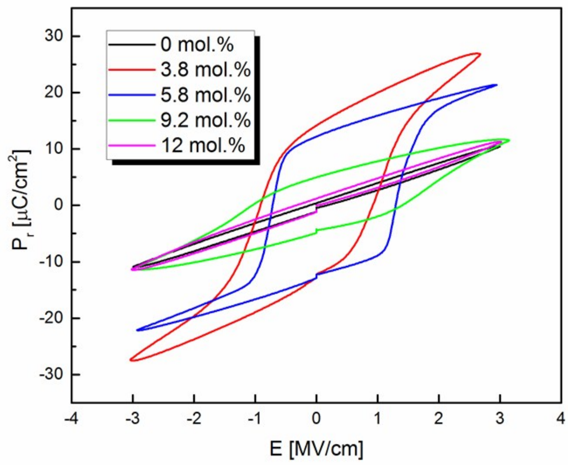

Figure S2. Hysteresis loops of different Y doping concentration samples.

S3. Ferroelectricity in a 5 nm thick HYO film.

As mentioned in the main text, the clear lattice image of 5 nm HYO film by HRTEM has indicated a well crystallized state of the film. To verify its ferroelectricity, pulse voltage test is measured and the result is shown in fig. S3. Fig. S3(a) shows the transient current during pulse triangular voltage wave and fig. S3(b) shows the hysteresis loop obtained by integration of the current with time. From fig. S3 we can get the conclusion that the 5 nm HYO film is also ferroelectric. Compared with the 15 nm ferroelectric HYO film, the 5 nm HYO film shows a bigger switchable polarization (2Pr) of 46 μC/cm² and a coercive field of around 1.3 MV/cm.

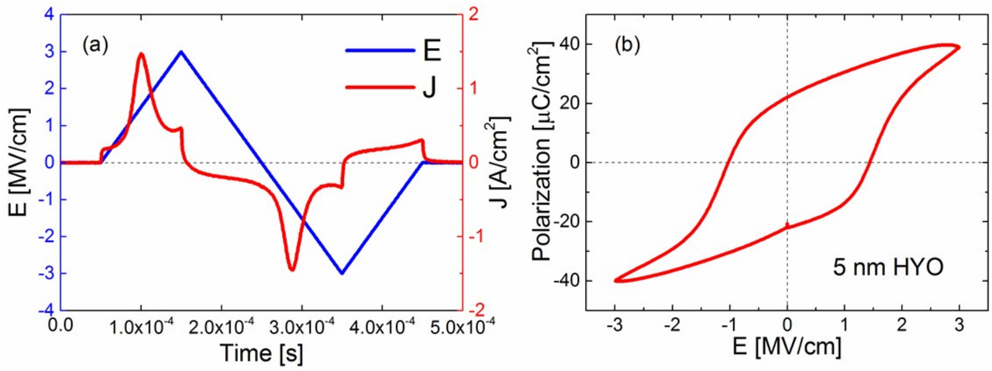

Figure S3. (a) Pulse voltage test of a 5 nm HYO capacitor. (b) Polarization-electric hysteresis loop of a HYO MIM capacitor.

S4. Fitting results of the slope of fatigue rate at different temperatures.

As mentioned in the main text, to avoid the wake-up presenting after 10^4 cycles measured at 353 K, we used data after 10^5 cycles (including 10^5 cycles) to fit the slope of fatigue rate at different temperatures and results are shown in fig. S4. The value of *R(T)* at each temperature is extracted from the slope of fitting lines, which changes from -0.14 at 323K to -0.23 at 423K. Then the value of activation energy E_a can be extracted and the results are shown in fig. 4f in the main text.

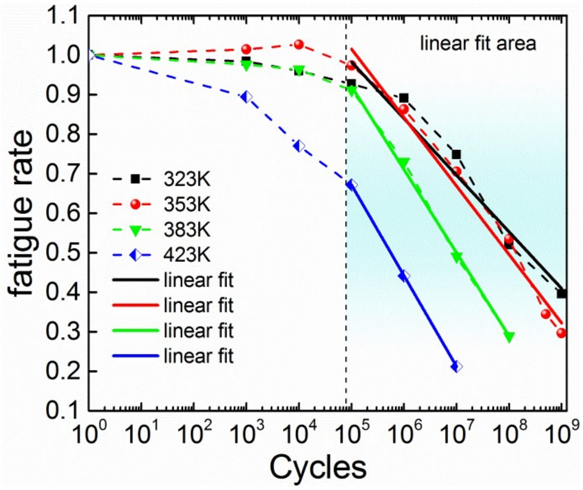

Figure S4. Fitting results of the slope of fatigue rate at different temperatures after 10^5 cycles (including 10^5 cycles).